RHEUMATOLOGY

Rheumatology 2010;49:915–923
doi:10.1093/rheumatology/keq033
Advance Access publication 25 February 2010

Original article

Aberrant localization of ezrin correlates with salivary acini disorganization in Sjögren's Syndrome

Paola Pérez[1], Sergio Aguilera[2], Nancy Olea[1], Cecilia Alliende[1], Claudio Molina[3], Mónica Brito[1], María-José Barrera[1], Cecilia Leyton[1], Anne Rowzee[4] and María-Julieta González[1]

Abstract

Objectives. To analyse whether the alterations in the structure and organization of microvilli in salivary acinar cells from SS patients are linked to changes in the expression and/or cellular localization of ezrin.

Methods. Salivary gland (SG) acini from controls and SS patients were used to evaluate ezrin expression by western blot and localization of total and activated (phospho-Thr567) ezrin by IF and EM.

Results. In acini from control labial SGs, ezrin was located predominantly at the apical pole and to a lesser extent at the basal region of these cells. Conversely, in acini extracts from SS patients, ezrin showed significantly elevated levels, which were accompanied with localization mostly at the basal region. Moreover, F-actin maintained its distribution in both the apical region and basolateral cortex; however, it was also observed in the acinar cytoplasm. Phospho-ezrin (active form) was located exclusively at the apical pole of acinar cells from control subjects and abundantly located at the basal cytoplasm in SS samples. These results were confirmed by immunogold studies.

Conclusions. The decrease of ezrin and phospho-ezrin at the apical pole and the cytoplasmic redistribution of F-actin suggest an altered interaction between the F-actin-cytoskeleton and plasma membrane in SS patient acini, which may explain the microvilli disorganization. These alterations could eventually contribute to SG hyposecretion in SS patients.

Key words: Ezrin, Cytoskeleton, Apical pole, Microvilli, Cell polarity, Hyposecretion, Salivary gland, Sjögren's syndrome.

Introduction

SS is a chronic autoimmune disease that affects up to 4 million Americans with an estimated incidence of 3–5% [1]. SS occurs primarily in women, with a 9 : 1 ratio over the occurrence in men. SS is clinically characterized by dry eyes and mouth [2]. Salivary and lachrymal hyposecretion in patients has been associated with various factors including autoantibodies against muscarinic-M3 receptors [3], acinar atrophy [4] and increased levels of cholinesterase [5]. However, in a significant number of SS patients with hyposecretion these alterations are absent, thus the correlation between the observed changes and dryness remains controversial [5, 6]. We reported previously that acini from SS patients present alterations in structural components of the acinar apical pole including a dilated lumen, loss of microvilli and structural changes in the remaining microvilli [7]. As the proteins involved in the exocytosis of secretory granules are localized in the apical pole of acinar cells, the study of this subcellular compartment is highly relevant for a better understanding of the hyposecretion suffered by SS patients.

Proteins of the ezrin, radixin and moesin family (ERM) are ubiquitous and co-localize with F-actin at cellular apical surfaces, such as filopodia, membrane ruffles and microvilli [8], providing a regulated link between the

[1]Program of Cell and Molecular Biology, ICBM, Faculty of Medicine, University of Chile, [2]INDISA Clinic, [3]Oral Pathology, Mayor University, Santiago, Chile and [4]NIDCR, National Institute of Health, Bethesda, MD, USA.

Submitted 2 September 2009; revised version accepted 19 January 2010.

Correspondence to: María-Julieta González, Institute of Biomedical Sciences, Faculty of Medicine, University of Chile, Casilla 70061, Santiago 7, Chile. E-mail: jgonzale@med.uchile.cl

BASIC SCIENCE

plasma membrane and the actin cytoskeleton [9]. Ezrin is expressed in epithelial cells where it associates with microvilli [10, 11]. Activation of ezrin is required for its binding to both membrane proteins and to the actin cytoskeleton. The transition from a closed to an open conformation is necessary to unmask binding sites (C-terminal, C-ERMAND; N-terminal N-ERMAND) [12]. Phosphorylation of threonine 567 (Phospho-Thr567) as well as interactions with phosphatidylinositol-4,5-bisphosphate (PIP2) open the dormant form, freeing the C-ERMAND to bind actin and the N-ERMAND to bind membrane proteins. This conformation is known as the 'active' form of ezrin [13]. In Ezrin$^{-/-}$ mice, the apical domains of intestinal and retinal pigment epithelial cells exhibit morphological defects [8, 14]. Particularly, ezrin knockdown in intestinal cells produces severe achlorhydria as a result of impaired formation of the canalicular apical membrane [15]. This evidence suggests that ezrin is essential for the morphogenesis and function of polarized epithelial cells. Considering the altered morphology of the apical pole of salivary gland (SG) acinar cell from SS patients [7], we compared the expression and localization of ezrin, P-ezrin and F-actin in SG acini from SS patients and control subjects to determine if changes in ezrin expression and/or activation are implicated in the alterations of the apical pole organization of acinar cells and could lead to gland hyposecretion in these individuals.

Materials and methods

Patients and biopsies

All subjects were informed about the aims and procedures of the study and signed a written informed consent. The Ethics Committee of the Faculty of Medicine, University of Chile, approved the study. The individuals were subject to a complete clinical analysis and selected for patient or control group as we previously described [16]. Twelve SS patients [mean age (range): 33 (22–55) years] were diagnosed according to the American–European Consensus criteria [17]. Nine control subjects [mean age (range): 52 (31–75) years] were selected from individuals who did not fulfil primary SS classification criteria. Labial SGs (LSGs) were surgically removed according to the procedure of Daniels [18] and kept briefly in cold phosphate-buffered saline (PBS) or snap-frozen in liquid nitrogen and stored at −80°C until processed.

Isolation of acini and ducts from LSGs

Acini and ducts were isolated from LSGs as previously described in Perez *et al*. [19].

Processing LSGs and isolated acini for confocal microscope analysis

Whole LSGs were fixed for 6 h in 1% paraformaldehyde in PBS pH 7.2, and processed according to standard protocols. Antigen retrieval was performed using 0.01 M citrate buffer, pH 6.0 at 90°C, for 20 min followed by 40 min at room temperature (RT). Isolated acini samples were fixed for 20 min in Trevor's fixative, then washed twice in 150 mM Tris–HCl, pH 7.4 and once in PBS; followed by incubation in 100% methyl alcohol for 10 min at −20°C and blocked with 0.25% casein–PBS. Acini were adhered to silane coated slides and incubated with primary antibodies diluted in 0.25% casein–PBS for 16 h at 4°C. To detect P-ezrin, samples were fixed in 10% TCA for 10 min at 4°C followed by 0.2% Triton X-100 for 10 min [20] followed by blocking with 0.25% casein–PBS before incubation with anti-phospho-ezrin antibody. Alexa-Fluor-conjugated secondary antibodies diluted in PBS were incubated on slides for 1 h at RT. Nuclei were visualized using 1 μg/ml propidium iodide, 1 μg/ml RNAse A in PBS, pH 7.4 for 1 min and F-actin was detected with Alexa-Fluor-546 phalloidin (Molecular Probes; Invitrogen, Eugene, OR, USA). Immunostained acini were mounted using 60% glycerol, 7% mowiol and 2% 1,4-diazabicyclo[2.2.2]octane (DABCO) and optical sections (0.8 μm) located at the middle of each acini were recorded using an LSM-140 Axiovert-10.0 confocal laser scanning microscope (Zeiss, Deutschland, Germany). Unrelated immunoglobulin was used as negative control.

Immunogold labelling and quantification

LSG samples from each patient were fixed at 4°C for 18 h in 4% paraformaldehyde, 0.2% picric acid, 0.5 M $CaCl_2$, 1% glutaraldehyde in PBS pH 7.4 and then rinsed overnight in PBS supplemented with 0.5 mM $CaCl_2$, 3.5% sucrose. Free aldehydes were blocked using 50 mM NH_4Cl in cacodylate buffer for 1 h at 0°C. Free phosphates were removed by washing samples four times for 15 min in 3.5% sucrose, 0.1 M sodium maleate, pH 6.5. The samples were stained in 2% uranyl acetate in 1% maleate buffer, pH 7.4 for 2 h at 0°C. Samples were then dehydrated in ethanol and embedded in resin LR Gold. Sections were obtained using a Porter–Blum ultramicrotome (Sorvall MT-2; Thermo Electron Corporation, Asheville, NC, USA) mounted over grids and processed for immunogold. Tissue sections were washed in Tris-buffered saline (TBS), blocked with 1% BSA, 0.1% Tween-20 in TBS for 10 min, and subsequently incubated with the primary anti-ezrin antibody diluted 1: 50 in TBS for 90 min at RT. Pre-immune mouse serum was used as a negative control. After washing in TBS the grids were incubated with secondary antibody conjugated to 15-nm gold particles for 1 h at RT. Sections were then stained with uranyl acetate and observed in transmission electron microscope (EM-109; Zeiss). Images were digitalized (SnapScan e5; Agfa-Gevaert N.V, Mortsel, Belgium). The relative distribution of immunogold signal in both the apical and basal cytoplasm in acinar cells was determined on at least five microphotographs from SS patients and controls. Microphotographs that contained acinar lumen or tight junctions (representing the apical pole) and nuclear matrix or cytoplasm (representing the basal pole of the cell) for each sample were analysed. The total density was obtained by counting gold particles number using J software (Rasband WS, NIH, Bethesda, MD, USA) in Golgi, rough endoplasmic reticulum, secretory granules,

mitochondria and the apical and the basolateral plasma membrane, including microvilli. The net gold particle number (total number of particles less background number of particles) was divided by the total area analysed (μm^2) to obtain the total particle density value (gold particles/μm^2). Finally, the percentage of gold particles in the apical and basal poles was calculated respective to the total particle density value.

Immunoblot analysis

To detect ezrin, pelleted acini were homogenized and protein extracts were obtained and processed for PAGE and immunoblot as was previously reported [21]. The anti-ezrin antibody was used at a 1:500 dilution in blocking buffer for 1 h at RT, washed three times 10 min in TBT and incubated with secondary antibodies at a dilution of 1:5000 for 1 h at RT. To detect phospho-ezrin, an aliquot of the acini suspension was incubated for 20 min at 4°C in 10% trichloroacetic acid (TCA). TCA was removed by washing with 150 mM Tris–HCl, pH 7.4 before homogenization. Ezrin and phospho-ezrin bands were analysed densitometrically (UN-Scan-IT; Silk Scientific Corporation, UT, USA) and values obtained were normalized to those of β-actin.

RT–PCR

Total RNA from the acini fraction of one control and three SS patients, was obtained using the RNeasy Mini Kit according to the manufacturer's instructions (Qiagen, Valencia, CA, USA). RNA quality was assessed and RT–PCR was performed according to Perez *et al*. [22]. The following specific primers for human ezrin were used: forward 5′-CAC GCT TGT GTC TTT AGT GCT TC-3′, reverse 5′-GCA TCT TGT ATC ACA CAG GC-3′. See details of reagents and antibodies in supplementary data (available at *Rheumatology* Online).

Statistical analysis

Normalized data were processed to calculate the mean (S.D.). Statistical analyses of the data were performed using descriptive statistics and Mann–Whitney test to assess the significance between groups. $P < 0.05$ was considered statistically significant.

Fig. 1 Ezrin localization in LSGs from SS patients and controls.

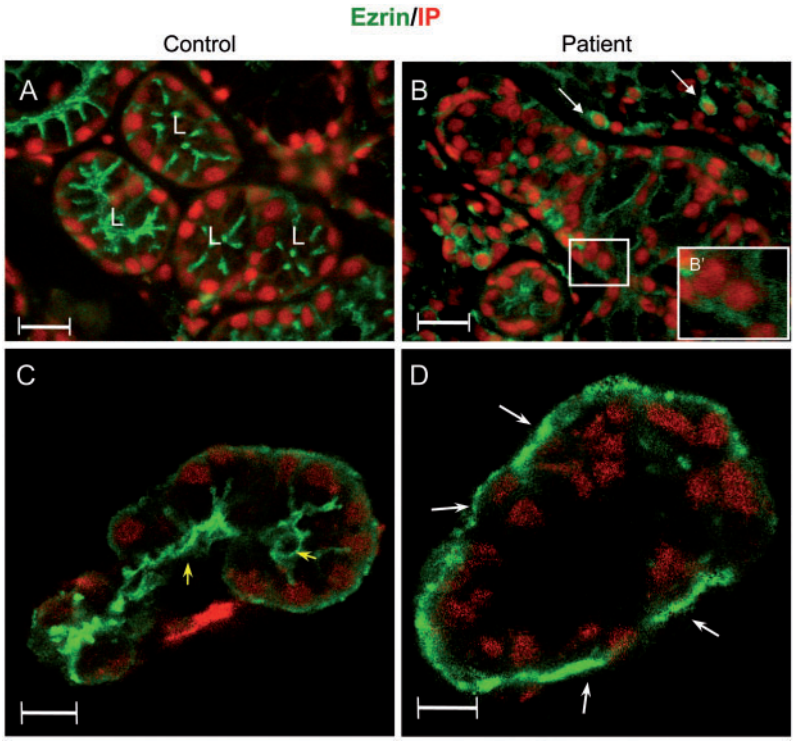

Indirect IF images of paraffin sections (**A**, **B**) and fresh acini adhered to glass slides (**C**, **D**) were incubated with a mouse antibody to human ezrin (green) and propidium iodide (PI, red) as described in the 'Materials and methods' section. (**A**) An LSG section from a control subject. (**B**) An LSG section from an SS patient. White arrows indicate inflammatory cells expressing ezrin. (**B′**) Boxed area in B showed at higher magnification (1.5×). (**C**, **D**) Confocal sections (0.8 μm) of representative acini from control (**C**) and SS patient (**D**). Yellow arrows indicate the location of acini lumen. White arrows indicate the changed location of ezrin immunoreactivity in the basal pole of the acini cells. Bars correspond to 15 μm.

Results

Ezrin localization in sections of LSGs and in acini

IF studies of glandular sections were performed to identify as to which cells expressed ezrin in LSGs, (Fig. 1A and B). Ezrin expression was not seen in myoepithelial, endothelial or fibroblast cells. In control samples, ezrin was detected in both acinar and ductal cells and was located mainly in the apical area of these cells, adjacent to the lumen (Fig. 1A). In SS patients, ezrin immunoreactivity was lower in the apical area and higher in basal cytoplasm (Fig. 1B and B′) and it was also detected in the cytoplasm of inflammatory cells (Fig. 1B, white arrows). As both epithelial and inflammatory cells express ezrin, we isolated a fraction enriched in acini from LSG to eliminate the ezrin produced by inflammatory cells. In acini from control subjects, intense immunoreactivity was observed at the apical surface with little to no reactivity in the basal cytoplasm (Fig. 1C). Conversely, the ezrin signal in acini from SS patients presented a marked intensity in the basal cytoplasm, but scarce immunoreactivity at the apical area (Fig. 1D).

Ezrin messenger RNA and protein levels in acinar cells

To analyse whether the changes observed in ezrin distribution in SS patients correlated with changes in ezrin gene expression and/or protein levels, RT–PCR and immunoblot assays were performed on epithelial cells. RT–PCR assays were performed using acinar cDNA from three SS patients and one control individual. Ezrin mRNA levels were higher in SS patients than in the control sample (Fig. 2A). Immunoblot analysis for ezrin identified a unique band of ~80 kDa in both the groups. Densitometric analysis demonstrated that ezrin protein levels in SS patients [0.59 (0.12)] were significantly higher ($P = 0.037$) than in controls [0.23 (0.1)] (Fig. 2B and C).

Localization and levels of active ezrin

The link between the actin-cytoskeleton and plasma membrane is considered a functional indicator of active ezrin [23], and therefore we performed confocal IF to determine if ezrin and F-actin co-localize in acini (Fig. 3A). In control acini, ezrin localization was coincident with zones having high reactivity for F-actin in the apical area of cells lining the lumen and in the basolateral cortex (Fig. 3A, control). In SS patients, ezrin was mainly located in the basal cytoplasm of acinar cells, whereas F-actin not only maintained its distribution in both the apical region and basolateral cortex, but it was also observed in the cytoplasm (Fig. 3A, patient). P-ezrin was detected exclusively in the apical surface of acinar cells from controls (Fig. 3B, control). On the contrary, in SS patients P-ezrin was observed mainly in the basal cytoplasm (Fig. 3B, patient). Furthermore, we observed strong co-localization between P-ezrin and total actin in the basal region of acini from SS patients (data not shown). The levels of P-ezrin were determined using immunoblot analysis of acinar protein extracts treated with TCA from 6 of 12 patients. In these analyses, three of the six SS patients studied demonstrated a decreased signal for P-ezrin

Fig. 2 Ezrin messenger RNA and protein levels in primary acini of LSGs from SS patients and healthy controls.

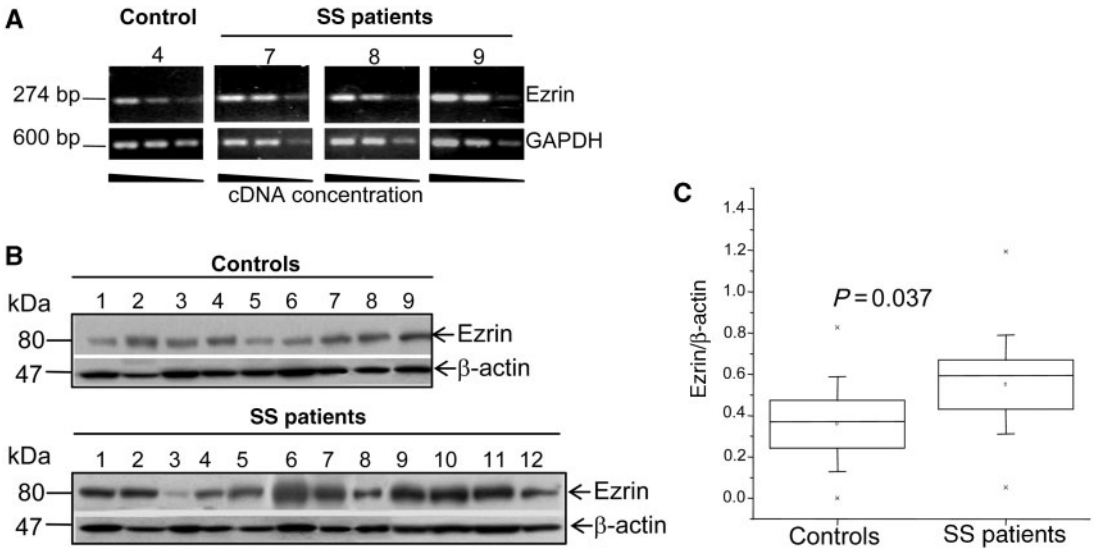

Total RNA and protein extracts from primary LSG epithelial cells were analysed by RT–PCR (**A**) and immunoblot (**B**, **C**). (**A**) For each subject, three different amounts of total RNA were used for RT–PCR (600, 300 and 60 ng). Ezrin was detected as a single band of 274 bp. Glyceraldehyde 3 phosphate dehydrogenase (GAPDH) was detected as a band of 650 bp. Samples from three SS patients and one control are shown. (**B**) Gland extracts were probed by immunoblotting for ezrin and β-actin (loading control). (**C**) Densitometry data of the immunoblot in (**B**). Ezrin signal was normalized against β-actin for each individual and graphed in box plots. Boxes indicate mean (S.D.) of three independent immunoblots.

Fig. 3 Localization and levels of P-ezrin and its relation with the actin cytoskeleton in acini of LSGs.

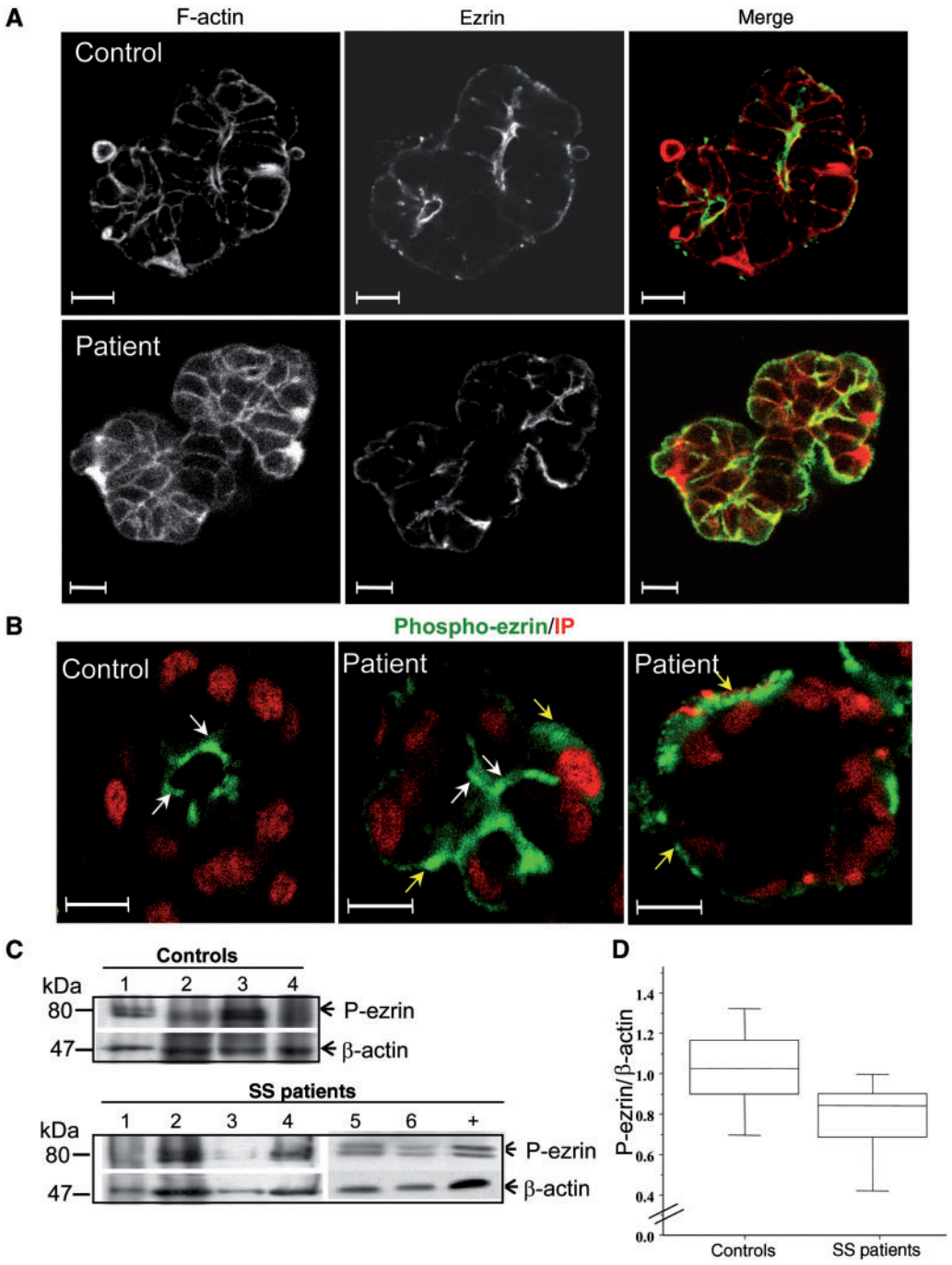

(**A**) Representative confocal IF images showing relation between ezrin (green) localization and F-actin (red) in acini from control and SS patient LSGs. (**B**) Representative confocal IF images showing the localization of P-ezrin (green) and nuclei (PI, red) in LSG acini from control and SS patients. Bars correspond to 10 μm. (**C**) Immunoblot analysis of P-ezrin and β-actin (loading control) in acini from SS patients ($n = 6$) and controls ($n = 4$). (**D**) Densitometry data of immunoblot in (**C**). P-ezrin signal was normalized against β-actin for each individual and graphed in box plots. Boxes indicate mean (S.D.) of the immunoblot.

(Fig. 3C). Statistical analyses showed a tendency towards a decrease in the ratio P-ezrin/β-actin in patients with respect to controls ($P = 0.05$; Fig. 3D).

Ultrastructural localization of ezrin in acini

Considering the limited resolution that IF provides, we performed immunogold assays to determine the subcellular localization of ezrin and its relationship with the ultrastructural organization of the apical pole in acinar cells with high resolution. In control samples, ezrin immunoreactivity was primarily associated with the apical microvilli (Fig. 4A); however, in SS patients a lower signal was observed only in the cytoplasm adjacent to the apical plasma membrane (Fig. 4B). This low-intensity ezrin signal was evident only in acini with disorganized microvilli compared with those with apparently normal microvilli from the same patient (data not shown). In addition, ezrin immunoreactivity in the basal cytoplasm of acinar cells from SS patients was notably higher than in controls (Fig. 4C and D). These results confirm the changes in ezrin distribution observed by IF, giving a better definition of subcellular ezrin location and specifically showing the changes observed in SS patients. Immunogold particles were quantified by determining their density in the apical microvilli and basolateral cytoplasm. The average signal density in the microvilli of SS patient acini was five times lower than that of controls (Fig. 4E). Conversely, the density of ezrin in the basal cytoplasm of acinar cells was eight times higher in SS patients than that in controls (Fig. 4E). Considering its structural function, the decreased presence of ezrin in the apical pole of the acinar cells of SS patients may explain the disruption of microvilli structure described previously in these patients [16]. To address whether the changes described involve additional proteins from the apical pole of the acinar cells, we evaluated the localization of two apical proteins, aquaporin 5 (AQP-5) and zonnula occludens 1 (ZO-1). AQP-5 is an integral plasma membrane protein channel that carries water into the acinar lumen, which is found on the apical membrane but not in the cytoplasm [24]. ZO-1 is a cytosolic protein that, like ezrin, interacts with proteins in the cellular membrane and is involved in organizing tight junctions and in some signalling pathways [25]. In patients and controls, AQP-5 was observed mostly at the apical surface; however, some acinar cells showed immunoreaction at the basal surface, corresponding to basal regions where ezrin also showed a high signal (see supplementary figure 1A and B available as supplementary data at *Rheumatology* Online). Thus, these results support previous reports of redistribution of the apico–basal polarity of AQP-5 in SS patients. ZO-1 showed the same location in patients and controls.

Discussion

We determined for the first time that ezrin expression in LSG acini from SS patients is higher than controls, displaying important changes in apico–basal cytoplasm distribution. The relocation of ezrin correlated with disrupted microvilli structures that were consistently observed in the LSGs of SS patients, additional changes in intensity and distribution of actin were also observed. These results suggest that the loss of ezrin in the apical pole generates an altered relationship between the actin cytoskeleton and the apical cellular membrane in acini, which could modify the exocytosis process in acinar cells of LSGs from SS patients.

We postulate two hypotheses to explain the changes in the location of ezrin in SS patients. First, the mechanisms that maintain the polarized localization of ezrin may be altered. Scarce evidence has been reported about the mechanisms of cytosolic protein sorting, but those described for the location of apical proteins may be used to help understand the cellular distribution of ezrin. For example, a polarized distribution of actin isoforms has been described in gastric parietal cells [26, 27]. Like ezrin, β-actin is located in the apical pole of parietal cells, whereas γ-actin is located in the basolateral cytoplasm [28]. It has been proposed that this polarized distribution of β-actin is generated by the local translation of its mRNA at the actin cytoskeleton [28]. If the normal mechanism that results in the apical localization of ezrin is dependent on the association of its mRNA with the cytoskeleton, then changes observed in the actin cytoskeleton may explain the loss of polarized ezrin in SS acini. A second explanation is that the apical location of ezrin is dependent on its interaction with proteins in the apical membrane. EBP50 is a scaffolding protein important in the organization of microvilli and in the location of ezrin in epithelial cells [29]. In intestinal epithelial cells from EBP50 knockout mice, ezrin is present mainly at the basal cytoplasm and is less often associated with the actin cytoskeleton. Furthermore, there is no detectable P-ezrin in the apical region of epithelial cells [30]. This finding suggests that the presence of EBP50 in the apical pole is necessary to maintain the location of ezrin. The location of EBP50 is now being studied in LSG acini from SS patients; preliminary results show distribution similar to ezrin, suggesting a tight functional association between both proteins (data not shown).

The redistribution of ezrin shown here in LSG acini has been described previously in lung, oesophageal and ovarian cancer tissues, and is consistently correlated with disorganized structures and loss of the differentiated phenotype [31–33]. There is evidence suggesting that subcellular redistribution of ezrin plays an important role during lung cell differentiation [34]. These observations suggest that ezrin may act as a membrane–cytoskeletal linker to strengthen the cell's capacity to maintain its normal differentiated phenotype [31, 32]. We have previously shown changes in the post-translational modifications in salivary MUC5B from SS patients [16]. If these changes are interpreted as part of a de-differentiation of acinar cells, the alterations here observed in ezrin may be part of this phenomenon. This hypothesis requires further investigation, since we do not know the mechanism involved in the ezrin redistribution in patients' acinar cells.

LSG acini from 10/12 SS patients showed increased levels of ezrin compared with controls. These data

Fig. 4 Immunoelectron microscopy localization of ezrin in sections of LSGs from control (**A**, **B**) and SS patients (**C**, **D**).

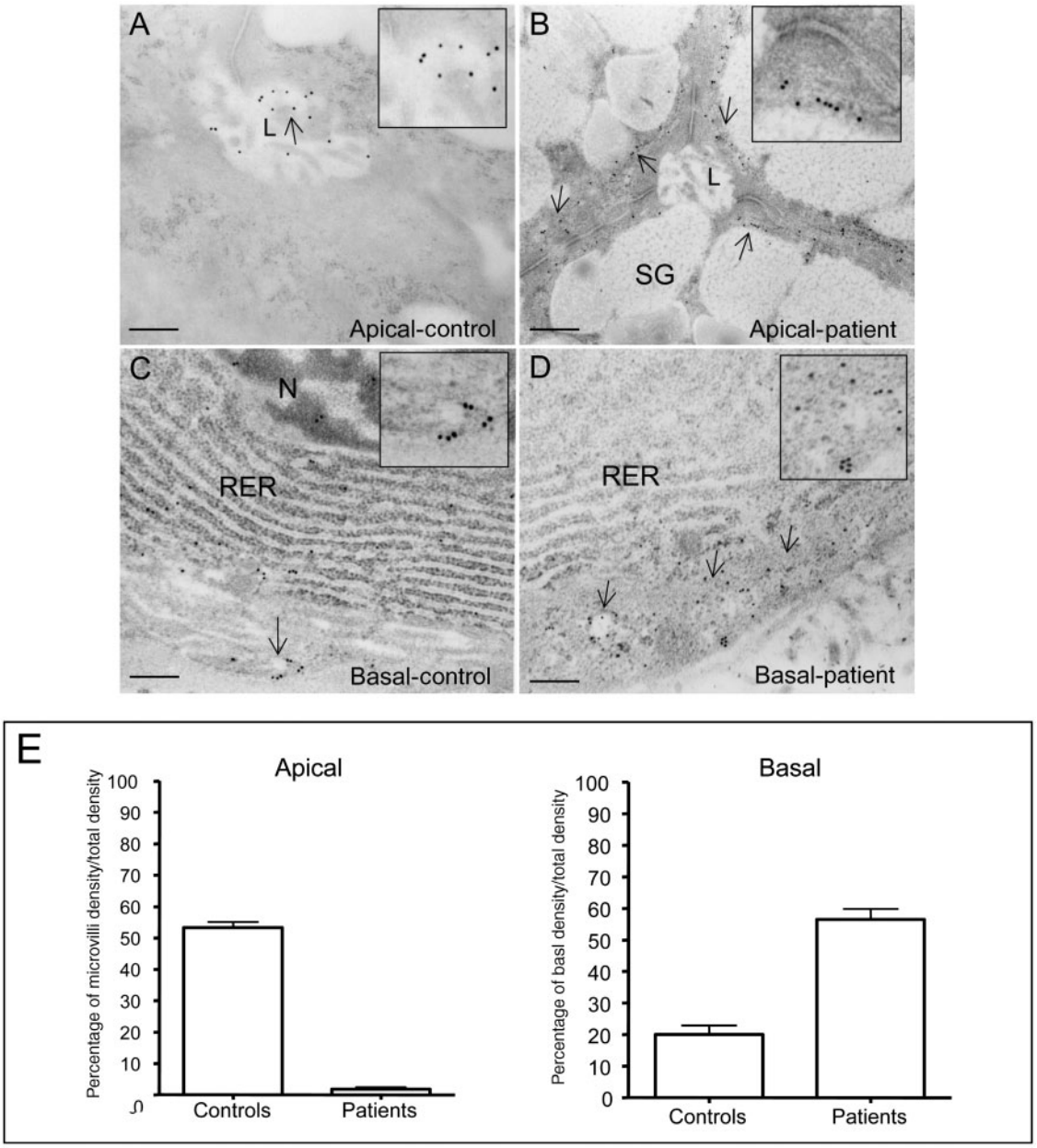

Representative images from the apical zone of acinar cells are shown secretory granules (SG), acinar lumen (L) and arrows indicate location of immunogold particles. (**A–D**) Insets show a higher magnification of immunogold particles. (**A**, **B** and **C**, **D**) Representative images from the apical and basal pole of acinar cells are shown, respectively. Rough endoplasmic reticulum (RER) and nucleus (N). Bars in (**A**) and (**C**) correspond to 0.2 μm and in (**B**) to 0.4 μm. (**E**) Quantification of the gold particle density in SS patients and controls. Graphs depict the particle density of microvilli in the apical pole or in the basal pole as a function of total particle density. Density is expressed as the amount of gold particles per quadratic micrometre and bars illustrate mean (S.D.) of two sections per patient.

suggest a compensatory up-regulation of ezrin gene expression in order to overcome defects in cytoskeletal organization in SS patients. Although much is known about ezrin function, there are few reports analysing the regulation of ezrin expression. Among the signals that have been related to ezrin overexpression are IL-11 and TNF-α [35, 36].

There is a trend towards decreased activation of ezrin in SS patients, even in the presence of higher levels of ezrin protein. Although these results are preliminary, we

suggest that ezrin expression and activation may be controlled by independent mechanisms. Neither the kinases implicated in the phosphorylation of ezrin nor the signals involved in maintaining the integrity of the microvilli have been analysed in the LSG. In endothelial cells, TNF-α produces significant changes in the organization of the cytoskeleton, which results in a decrease in ezrin phosphorylation by protein kinase C (PKC) [35, 37]. Immunohistochemistry studies of the LSGs of SS patients have shown a decrease in the expression for PKC-α and -βII [38], and overexpression of TNF-α [39]. A TNF-α-dependent decrease in the activity of PKC-α could explain the decrease in P-ezrin levels seen in SS patients.

In summary, our results support the hypothesis that relocation of ezrin may be involved in the disruption of microvilli at the apical pole of LSG acini in SS patients. Considering that the molecular machinery of exocytosis is located in this domain of the plasma membrane, the changes observed here could eventually be related to the hyposecretion suffered by SS patients.

Rheumatology key messages

- An aberrant localization of ezrin in salivary acinar cells from SS patients was observed.
- Subcellular localization changes of active ezrin could explain the modifications of microvilli organization observed.

Acknowledgement

The authors thank Dr Jorge Sans Puroja (Unidad de Análisis Celular Integral, CESAT, ICBM, Facultad de Medicina, Universidad de Chile, Santiago, Chile) for assistance in confocal studies. M.-J.G. had full access to all of the data in the study and takes responsibility for the integrity of the data and the accuracy of the data analysis. P.P., S.A., M.-J.G.: study design; P.P., S.A., P.P., M.B., N.O., M.-J.B., M.-J.G.: acquisition of data; P.P., M.B., N.O., M.-J.B., C.M., C.A., C.L., M.-J.G.: analysis and interpretation of data; P.P., M.-J.G., A.R., C.M., S.A.: Manuscript preparation; C.M., M.-J.G.: Statistical analysis.

Funding: Supported by grants (to M.-J.G., S.A. and C.M.) FONDECYT-CHILE 1080006, 1050192. P.P. and M.B. were supported by PhD fellowships granted by Conicyt, Mecesup-Postgrade University of Chile 99-03.

Disclosure statement: The authors have declared no conflicts of interest.

Supplementary data

Supplementary data are available at *Rheumatology* Online.

References

1 Manoussakis MN, Kapsogeorgou EK. The role of epithelial cells in the pathogenesis of Sjogren's syndrome. Clin Rev Allergy Immunol 2007;32:225–30.

2 Anaya JM, Talal N. Sjogren's syndrome comes of age. Semin Arthritis Rheum 1999;28:355–9.

3 Dawson LJ, Stanbury J, Venn N, Hasdimir B, Rogers SN, Smith PM. Antimuscarinic antibodies in primary Sjogren's syndrome reversibly inhibit the mechanism of fluid secretion by human submandibular salivary acinar cells. Arthritis Rheum 2006;54:1165–73.

4 Fox RI, Tornwall J, Michelson P. Current issues in the diagnosis and treatment of Sjogren's syndrome. Curr Opin Rheumatol 1999;11:364–71.

5 Dawson LJ, Fox PC, Smith PM. Sjogren's syndrome—the non-apoptotic model of glandular hypofunction. Rheumatology 2006;45:792–8.

6 Dawson L, Tobin A, Smith P, Gordon T. Antimuscarinic antibodies in Sjogren's syndrome: where are we, and where are we going? Arthritis Rheum 2005;52:2984–95.

7 Goicovich E, Molina C, Perez P *et al*. Enhanced degradation of proteins of the basal lamina and stroma by matrix metalloproteinases from the salivary glands of Sjogren's syndrome patients: correlation with reduced structural integrity of acini and ducts. Arthritis Rheum 2003;48:2573–84.

8 Saotome I, Curto M, McClatchey AI. Ezrin is essential for epithelial organization and villus morphogenesis in the developing intestine. Dev Cell 2004;6:855–64.

9 Mangeat P, Roy C, Martin M. ERM proteins in cell adhesion and membrane dynamics. Trends Cell Biol 1999; 9:187–92.

10 Berryman M, Gary R, Bretscher A. Ezrin oligomers are major cytoskeletal components of placental microvilli: a proposal for their involvement in cortical morphogenesis. J Cell Biol 1995;131:1231–42.

11 Berryman M, Franck Z, Bretscher A. Ezrin is concentrated in the apical microvilli of a wide variety of epithelial cells whereas moesin is found primarily in endothelial cells. J Cell Sci 1993;105(Pt 4):1025–43.

12 Fievet BT, Gautreau A, Roy C *et al*. Phosphoinositide binding and phosphorylation act sequentially in the activation mechanism of ezrin. J Cell Biol 2004;164:653–9.

13 Fiévet BB, Louvard DD, Arpin MM. ERM proteins in epithelial cell organization and functions. Biochim Biophys Acta 2007;1773:653–60.

14 Bonilha VL, Rayborn ME, Saotome I, McClatchey AI, Hollyfield JG. Microvilli defects in retinas of ezrin knockout mice. Exp Eye Res 2006;82:720–9.

15 Tamura A, Kikuchi S, Hata M *et al*. Achlorhydria by ezrin knockdown: defects in the formation/expansion of apical canaliculi in gastric parietal cells. J Cell Biol 2005;169: 21–8.

16 Alliende C, Kwon YJ, Brito M *et al*. Reduced sulfation of muc5b is linked to xerostomia in patients with Sjogren syndrome. Ann Rheum Dis 2008;67:1480–7.

17 Vitali C, Bombardieri S, Jonsson R *et al*. Classification criteria for Sjogren's syndrome: a revised version of the European criteria proposed by the American-European Consensus Group. Ann Rheum Dis 2002;61:554–8.

18 Daniels TE. Labial salivary gland biopsy in Sjögren's syndrome. Assessment as a diagnostic criterion in 362 suspected cases. Arthritis Rheum 1984;27:147–56.

19 Perez P, Anaya JM, Aguilera S *et al*. Gene expression and chromosomal location for susceptibility to Sjogren's syndrome. J Autoimmun 2009;33:99–108.

20 Hayashi K, Yonemura S, Matsui T, Tsukita S. Immunofluorescence detection of ezrin/radixin/moesin (ERM) proteins with their carboxyl-terminal threonine phosphorylated in cultured cells and tissues. J Cell Sci 1999;112(Pt 8):1149–58.

21 Kwon YJ, Perez P, Aguilera S *et al*. Involvement of specific laminins and nidogens in the active remodeling of the basal lamina of labial salivary glands from patients with Sjogren's syndrome. Arthritis Rheum 2006;54:3465–75.

22 Perez P, Kwon YJ, Alliende C *et al*. Increased acinar damage of salivary glands of patients with Sjogren's syndrome is paralleled by simultaneous imbalance of matrix metalloproteinase 3/tissue inhibitor of metalloproteinases 1 and matrix metalloproteinase 9/tissue inhibitor of metalloproteinases 1 ratios. Arthritis Rheum 2005;52:2751–60.

23 Bretscher A. Regulation of cortical structure by the ezrin-radixin-moesin protein family. Curr Opin Cell Biol 1999;11:109–16.

24 Delporte C. Aquaporins in secretory glands and their role in Sjögren's syndrome. Handb Exp Pharmacol 2009;190:185–201.

25 Fanning AS, Little BP, Rahner C, Utepbergenov D, Walther Z, Anderson JM. The unique-5 and -6 motifs of ZO-1 regulate tight junction strand localization and scaffolding properties. Mol Biol Cell 2007;18:721–31.

26 Goldenring JR. Pools of actin in polarized cells: some filaments are more stable than others Focus on 'Functionally distinct pools of actin in secretory cells'. Am J Physiol Cell Physiol 2001;281:C386–7.

27 Ammar DA, Nguyen PN, Forte JG. Functionally distinct pools of actin in secretory cells. Am J Physiol Cell Physiol 2001;281:C407–17.

28 Yao X, Chaponnier C, Gabbiani G, Forte JG. Polarized distribution of actin isoforms in gastric parietal cells. Mol Biol Cell 1995;6:541–57.

29 Morales FC, Takahashi Y, Kreimann EL, Georgescu MM. Ezrin-radixin-moesin (ERM)-binding phosphoprotein 50 organizes ERM proteins at the apical membrane of polarized epithelia. Proc Natl Acad Sci USA 2004;101:17705–10.

30 Reczek D, Berryman M, Bretscher A. Identification of EBP50: a PDZ-containing phosphoprotein that associates with members of the ezrin-radixin-moesin family. J Cell Biol 1997;139:169–79.

31 Tokunou M, Niki T, Saitoh Y, Imamura H, Sakamoto M, Hirohashi S. Altered expression of the ERM proteins in lung adenocarcinoma. Lab Invest 2000;80:1643–50.

32 Zeng H, Xu L, Xiao D *et al*. Altered expression of ezrin in esophageal squamous cell carcinoma. J Histochem Cytochem 2006;54:889–96.

33 Moilanen J, Lassus H, Leminen A, Vaheri A, Butzow R, Carpen O. Ezrin immunoreactivity in relation to survival in serous ovarian carcinoma patients. Gynecol Oncol 2003;90:273–81.

34 Huang T, You Y, Spoor MS *et al*. Foxj1 is required for apical localization of ezrin in airway epithelial cells. J Cell Sci 2003;116:4935–45.

35 Kishore R, Qin G, Luedemann C *et al*. The cytoskeletal protein ezrin regulates EC proliferation and angiogenesis via TNF-alpha-induced transcriptional repression of cyclin A. J Clin Invest 2005;115:1785–96.

36 Jiang WG, Hiscox S. Cytokine regulation of ezrin expression in the human colon cancer cell line HT-29. Anticancer Res 1996;16:861–5.

37 Koss M, Pfeiffer GR 2nd, Wang Y *et al*. Ezrin/radixin/moesin proteins are phosphorylated by TNF-alpha and modulate permeability increases in human pulmonary microvascular endothelial cells. J Immunol 2006;176:1218–27.

38 Tornwall J, Konttinen YT, Tuominen RK, Tornwall M. Protein kinase C expression in salivary gland acinar epithelial cells in Sjogren's syndrome. Lancet 1997;349:1814–5.

39 Fox PC, Brennan M, Di Sun P. Cytokine expression in human labial minor salivary gland epithelial cells in health and disease. Arch Oral Biol 1999;44(Suppl. 1):S49–52.